Cell, Vol. 119, 719–732, November 24, 2004, Copyright ©2004 by Cell Press

A Behavioral Role for Dendritic Integration: HCN1 Channels Constrain Spatial Memory and Plasticity at Inputs to Distal Dendrites of CA1 Pyramidal Neurons

Matthew F. Nolan,[1] Gaël Malleret,[1] Josh T. Dudman,[1] Derek L. Buhl,[2] Bina Santoro,[1] Emma Gibbs,[1] Svetlana Vronskaya,[1] György Buzsáki,[2] Steven A. Siegelbaum,[1,3,5,6] Eric R. Kandel,[1,4,5,6,*] and Alexei Morozov[1,7]

[1]Center for Neurobiology and Behavior
Columbia University
New York, New York 10032

[2]Center for Molecular and Behavioral Neuroscience
Rutgers University
Newark, New Jersey 07102

[3]Department of Pharmacology

[4]Departments of Physiology, Biochemistry and Biophysics, and Psychiatry

[5]Howard Hughes Medical Institute

[6]Kavli Institute for Brain Sciences
Columbia University
New York, New York 10032

[7]Unit of Behavioral Genetics
National Institute of Mental Health
Bethesda, Maryland 20892

Summary

The importance of long-term synaptic plasticity as a cellular substrate for learning and memory is well established. By contrast, little is known about how learning and memory are regulated by voltage-gated ion channels that integrate synaptic information. We investigated this question using mice with general or forebrain-restricted knockout of the *HCN1* gene, which we find encodes a major component of the hyperpolarization-activated inward current (I_h) and is an important determinant of dendritic integration in hippocampal CA1 pyramidal cells. Deletion of HCN1 from forebrain neurons enhances hippocampal-dependent learning and memory, augments the power of theta oscillations, and enhances long-term potentiation (LTP) at the direct perforant path input to the distal dendrites of CA1 pyramidal neurons, but has little effect on LTP at the more proximal Schaffer collateral inputs. We suggest that HCN1 channels constrain learning and memory by regulating dendritic integration of distal synaptic inputs to pyramidal cells.

Introduction

Considerable progress has been made toward identifying the molecular mechanisms mediating long-term, activity-dependent synaptic modifications thought to be important for memory storage (Bliss and Collingridge, 1993; Bliss et al., 2003; Milner et al., 1998). However, to alter neuronal output these synaptic changes must be read out by the integrative properties of the postsynaptic cell. Voltage-gated channels active at subthreshold potentials are ideally situated to influence this readout and to regulate the learning of new information by gating the initiation of somatic or dendritic spikes that serve as associative signals for the induction of synaptic plasticity (Bi and Poo, 1998; Golding et al., 2002; Magee and Johnston, 1997; Markram et al., 1997). At present, however, little is known about how these active integrative properties may control learning and memory.

We have focused our attention on the integrative role of the HCN1 channel subunit, one of four HCN (hyperpolarization-activated, cyclic-nucleotide gated, cation nonselective) subunits that generate hyperpolarization-activated inward currents (I_h) (Robinson and Siegelbaum, 2003). HCN1 is highly expressed in cerebellar cortical neurons and in pyramidal cells of the neocortex and hippocampus (Lorincz et al., 2002; Notomi and Shigemoto, 2004; Santoro et al., 2000). We previously found that knockout of the *HCN1* gene causes profound deficits in motor learning that may be accounted for by actions of HCN1 in cerebellar Purkinje cells (Nolan et al., 2003). In these spontaneously spiking neurons, HCN1 is activated by inputs that hyperpolarize the membrane below the threshold for spontaneous spiking. By stabilizing the integrative properties of Purkinje cells, HCN1 enables reliable encoding of information independently of their previous history of activity (Nolan et al., 2003). Here we ask, is HCN1 generally required in neuronal circuits important for learning and memory? Does it always play a permissive role, as it does in motor learning? Or does its function vary, depending on its cellular context?

To approach these questions, we have studied the role of HCN1 in forebrain pyramidal neurons. Unlike Purkinje cells, these neurons are generally not spontaneously active in the absence of synaptic input. Pyramidal neurons also have resting potentials substantially more negative than those of Purkinje cells. As a result, a significant fraction of I_h in pyramidal cells is activated at rest and therefore can contribute to the integration of postsynaptic potentials. The importance of HCN1 in synaptic integration in pyramidal neurons is underscored by its distinctive dendritic gradient of expression, with levels in apical dendrites increasing steeply as a function of distance from the soma (Lorincz et al., 2002). The resulting gradient of I_h density is thought to reduce the amplitude and duration of distal synaptic potentials and to remove the location dependence of synaptic summation that would otherwise arise as a result of the passive cable properties of the dendritic tree (Berger et al., 2001; Magee, 1998, 1999; Williams and Stuart, 2000, 2003).

The dendritic gradient of I_h is of further interest because different regions of the apical dendritic tree receive inputs from different sources. The most distal dendritic regions of pyramidal cells in CA1 contain the highest density of HCN1 channels and are innervated by direct perforant path (temporoammonic) inputs from layer III of the entorhinal cortex. These inputs may be of particular functional importance for representation of spatial information by CA1 neurons (Brun et al., 2002). The more proximal regions of the apical dendrite, where the HCN1 density is lower, are innervated by Schaffer

*Correspondence: erk5@columbia.edu

collateral inputs to CA1 from hippocampal CA3 neurons. Consistent with this lower channel density, pharmacological blockade of I_h does not alter long-term potentiation (LTP) or long-term depression (LTD) at the Schaffer collateral synapses (Gasparini and DiFrancesco, 1997; Wang et al., 2003). Given the high density of HCN1 at the distal perforant path inputs, we were interested in determining whether this channel may selectively regulate synaptic transmission and plasticity at these direct cortical inputs (Colbert and Levy, 1993; Remondes and Schuman, 2002).

Using mice with general (*HCN1*$^{-/-}$) and forebrain-restricted (*HCN1*$^{f/f,cre}$) knockout of the *HCN1* gene, we examined the influence of HCN1 channels on CA1 pyramidal cell physiology, synaptic integration and induction of LTP at inputs to CA1 pyramidal cells, as well as hippocampal network activity, and hippocampal-dependent forms of learning and memory. We provide evidence that HCN1 channels oppose LTP at perforant path inputs to pyramidal cells with no change in LTP at Schaffer collateral inputs, suppress theta frequency network activity, and constrain spatial learning and memory. Modified dendritic integration resulting in enhanced LTP at perforant path synapses provides a possible mechanism for enhanced learning by *HCN1*$^{f/f,cre}$ mice.

Results

Deletion of HCN1 Channels from Forebrain Neurons

We examined two HCN1 mutant mouse lines (Nolan et al., 2003): *HCN1*$^{-/-}$ mice in which HCN1 is deleted from the entire mouse and *HCN1*$^{f/f,cre}$ mice in which deletion of HCN1 is limited to the forebrain. Wild-type (*HCN1*$^{+/+}$) and floxed (*HCN1*$^{f/f}$) mice, used as littermate controls for experiments with *HCN1*$^{-/-}$ and *HCN1*$^{f/f,cre}$ mice, respectively, expressed HCN1 mRNA and protein with similar patterns to that described previously for wild-type mice (Lorincz et al., 2002; Santoro et al., 1997, 2000). In the forebrain, high expression of HCN1 mRNA was found in layer V of the neocortex and in the pyramidal layer of the hippocampus, with corresponding dense labeling of the protein occurring in regions containing the distal apical dendrites of pyramidal cells. By contrast, HCN1 mRNA and protein were absent from the brains of *HCN1*$^{-/-}$ mice and greatly reduced from the forebrain of *HCN1*$^{f/f,cre}$ mice (Nolan et al., 2003; Supplemental Figure S1 at http://www.cell.com/cgi/content/full/119/5/719/DC1/).

Contribution of Forebrain HCN1 Channels to Behaviors Involving Learning and Memory

We previously found that *HCN1*$^{-/-}$ mice have a profound deficit in motor learning. Thus, on the first 2 days of a water maze experiment in which mice learn to navigate to a submerged platform, whose location is indicated by a flag, these mice do not learn to swim directly to the platform but instead maintain a tendency to swim in loops (Nolan et al., 2003). By contrast, *HCN1*$^{f/f,cre}$ mice do not appear to have any deficits in motor learning and their performance in this visible platform phase of the water maze experiment was comparable to control (*HCN1*$^{f/f}$) mice (Figure 1A).

HCN1 Constrains Acquisition of a Spatial Memory Task

We next asked if deletion of HCN1 from forebrain neurons alters the performance of tasks requiring spatial learning. The submerged unmarked platform was placed in a new location that could only be determined by the mouse using spatial cues placed around the room and which remained the same during subsequent trials. A priming procedure, during which mice were placed on the platform at the new location for 15 s, was carried out 15 min prior to the first spatial learning trial. Mice were then trained with four trials per day over 4 days. Comparison of the performance of the mice on each day indicated that *HCN1*$^{f/f,cre}$ mice learned the spatial task faster than control mice, although both groups of mice reached a similar final level of performance and performed similarly when their memory of the platform location was tested with a probe trial indicating that they both use a spatial strategy to solve the task (Figure 1B). Comparison of swimming speed, time spent floating, or thigmotaxis did not reveal any effect of forebrain deletion of HCN1 during training on days 3–6, indicating that motor or motivational effects do not contribute to the differences in learning (Supplemental Figure S2A on the *Cell* website).

The short-term effects of information remembered during the 15 min between trials can be distinguished from long-term effects of memory storage between days by comparing the performance of control and *HCN1*$^{f/f,cre}$ mice across individual trials, rather than days (Figure 1C). During the four training trials of the first spatial training day (day 3), the path length for *HCN1*$^{f/f,cre}$ mice to reach the platform was consistently shorter than for *HCN1*$^{f/f}$ mice. Remarkably, this enhancement was visible during the first trial. However, the largest difference between the two groups of mice was on trial 1 of day 4, during which the performance of *HCN1*$^{f/f,cre}$ mice was significantly enhanced compared with *HCN1*$^{f/f}$ mice ($p = 0.01$). This is because the performance of *HCN1*$^{f/f}$ mice returned toward the pre-training level on the first trial of day 4 compared with the final trial of day 3, suggesting that the memory of the platform location used to complete the final trial on day 3 was poorly retained overnight by the *HCN1*$^{f/f}$ mice. By contrast, *HCN1*$^{f/f,cre}$ mice maintained a similar level of performance between these two trials, indicating that they retained the memory of the platform location from the previous day.

HCN1 Constrains Performance of Long-Term Components of a Water Maze Spatial Memory Task when Training Frequency Is Reduced

To determine if HCN1 channels also influence longer-term memory processes that operate cumulatively over several days, we examined the performance of the same group of mice on a more demanding task in which they were trained to find a hidden platform with only one trial per day (Figure 1D). The platform was placed in a new location and approximately 15 min before the first trial the priming procedure was again carried out. The path length for *HCN1*$^{f/f,cre}$ mice to reach the platform was reduced compared with *HCN1*$^{f/f}$ mice on both the first day and on days 5–8, indicating that deletion of HCN1

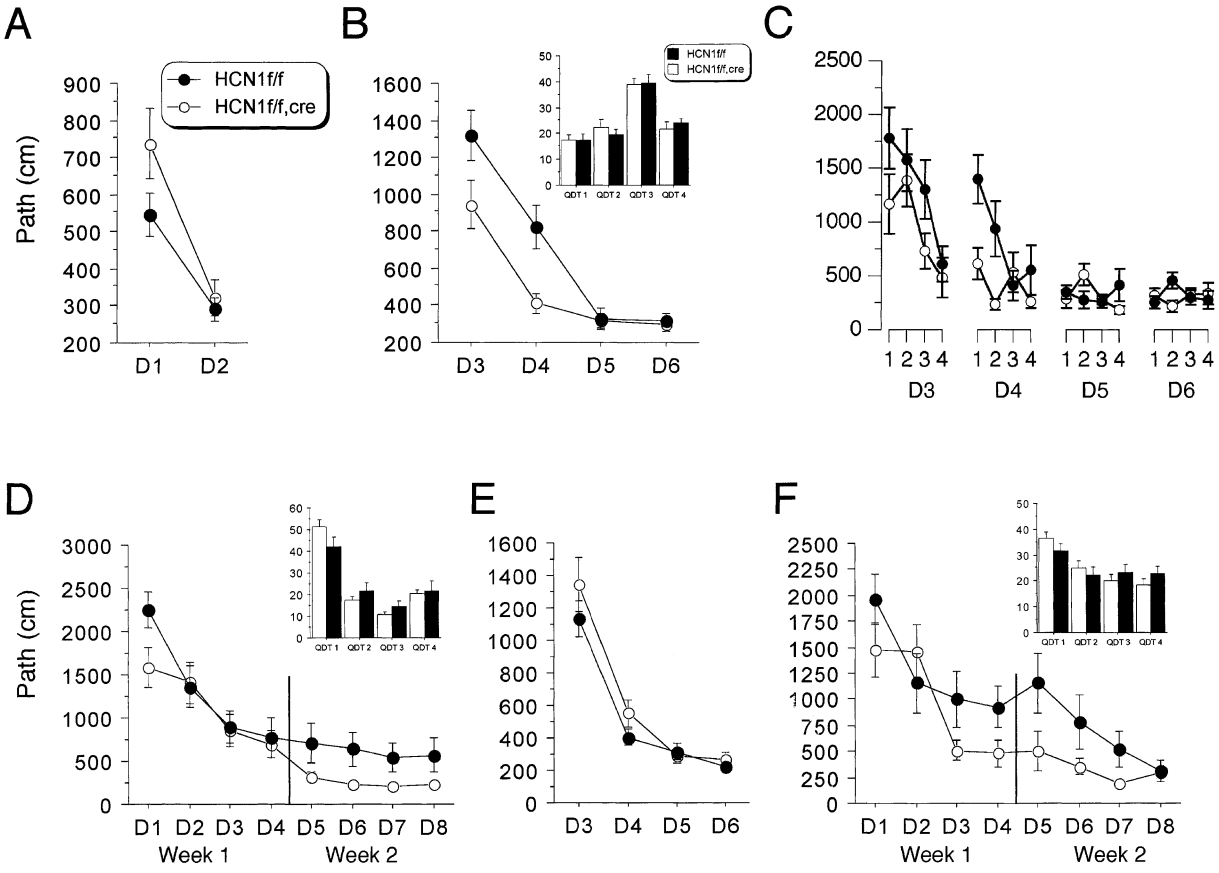

Figure 1. Short- and Long-Term Memory Is Enhanced by Deletion of HCN1 from Forebrain Neurons

The path length for mice to reach the platform in a water maze is plotted against the day of the experiment (D) or the trial number (T). The insets show the percentage of time spent in each quadrant of the pool during the corresponding probe trial.

(A) Data from the visible platform, nonspatial version of the water maze task (effect of genotype $p > 0.05$).

(B) The path length plotted against the day of the experiment for a four trials a day, hidden platform, spatial version of the water maze task. ANOVA indicated a significant difference between *HCN1*$^{f/f,cre}$ ($n = 13$) compared with *HCN1*$^{f/f}$ mice ($n = 12$) in path length and latency [$F(1,24) = 9.48$, $p = 0.005$ for path length; $F(1,24) = 7.05$, $p = 0.01$ for latency]. Probe trial performance on day 7 was similar in both groups of mice ($p = 0.29$).

(C) The data from the same experiment as in (B) plotted as a function of the trial number on each day.

(D) Data from a one trial per day, hidden platform version of the water maze task. The path length for *HCN1*$^{f/f,cre}$ mice to reach the platform on the first session was reduced compared with *HCN1*$^{f/f}$ mice ($p = 0.04$). The path length (genotype effect $p = 0.03$) and latency (genotype effect $p = 0.04$) for *HCN1*$^{f/f,cre}$ mice to reach the platform was also reduced during the second week of testing.

(E) Data from a different group of mice with a four trials a day, hidden platform version of the water maze task, without priming prior to the first trial on day 1. There was no significant difference between *HCN1*$^{f/f}$ mice ($n = 13$) and *HCN1*$^{f/f,cre}$ mice ($n = 14$) (ANOVA, latency $p = 0.21$, path $p = 0.19$).

(F) Data from the same group of mice as in (E) tested with one trial a day hidden platform water maze task, without priming. Forebrain deletion of HCN1 enhanced performance of the mice during the second week of the experiment (genotype effect of ANOVA for 2nd week, path length $p = 0.031$, latency $p = 0.028$).

enhances performance of short- and long-term components of the task.

The Enhancement of Short-Term, but not Long-Term, Memory Requires that the Mice Be Primed Prior to the First Trial

We next asked if the modulation by HCN1 of short- and long-term components of learning could be dissociated from one another. We repeated the water maze experiments in a second group of animals, but without the priming procedure (Figures 1E and 1F). In this case there was no significant difference between the performance of control and *HCN1*$^{f/f,cre}$ littermates when trained in the water maze task with four trials per day (Figure 1E). When the same mice were then trained to find the platform in a new location with one trial per day, again without the priming procedure, the early enhancement of learning by the *HCN1*$^{f/f,cre}$ mice was again absent (Figure 1F). However, the performance of *HCN1*$^{f/f,cre}$ mice was enhanced on days 5 to 7 of the experiment (Figure 1F). A probe trial after day 8 did not reveal a significant difference between the *HCN1*$^{f/f}$ and *HCN1*$^{f/f,cre}$ mice, indicating that both groups of mice use spatial strategies to solve the task.

These data suggest that forebrain HCN1 channels modulate both short- and long-term memory. The reduced path length to reach the hidden platform during

the initial trial following priming suggests that *HCN1*$^{f/f,cre}$ mice have an improved memory for information obtained during the priming procedure. The priming-independent, reduced path length to the hidden platform during later trials of the more difficult one trial per day experiment suggests that *HCN1*$^{f/f,cre}$ mice also have enhanced long-term memory.

Anxiety, Attention, and Fear Conditioning Are Not Altered by Deletion of HCN1 from Forebrain Neurons

Can the enhanced spatial learning shown by the *HCN1*$^{f/f,cre}$ mice be accounted for by changes in anxiety or attention? There was no significant difference between the behavior of *HCN1*$^{f/f,cre}$ and control mice in an elevated plus maze indicating that the two groups of mice do not differ in levels of anxiety. Nor was there a difference in pre-pulse inhibition, a simple test of sensory-motor gating, suggesting that basal attention is similar in the two groups of mice (Supplemental Figures S2B and S2C).

Does the spatial learning enhancement extend to other forms of learning and memory? We found no difference between *HCN1*$^{f/f,cre}$ and control mice in cued fear conditioning, an amygdala-dependent form of memory, or in a contextual-fear conditioning task, which is thought to involve a ventral hippocampal-dependent form of memory (Supplemental Figures S2D and S2E). Thus, the enhancement of learning and memory in *HCN1*$^{f/f,cre}$ mice does not appear to extend to contextual fear conditioning or to involve changes in anxiety or attention.

Effect of HCN1 Deletion on Hippocampal Network Activity: Enhancement of Theta Band Network Activity In Vivo

What is the neuronal basis for the enhancement of spatial learning? We focused our electrophysiological analysis on the CA1 region of the hippocampus, based on its importance for spatial learning and memory and the strong expression of HCN1 in this region. Since I_h has been suggested to influence network oscillations that may play important roles in learning and memory (Fisahn et al., 2002; Hu et al., 2002; Lupica et al., 2001; Maccaferri and McBain, 1996), we asked if deletion of HCN1 modifies hippocampal network oscillations. Delta, theta, gamma, and fast ("ripple") oscillatory field potentials were recorded in vivo from the CA1 pyramidal layer. Spectral analysis of the spontaneous field potentials recorded during slow wave sleep revealed no significant differences between *HCN1*$^{-/-}$ and *HCN1*$^{+/+}$ mice. Both low-frequency power and fast "ripple" power were remarkably similar (see Supplemental Figure S3). However, power in the theta frequency band (4–9 Hz), reflecting oscillations thought to be important in encoding and storing spatial information, was selectively enhanced in *HCN1*$^{-/-}$ animals during both wheel running ($p < 0.01$) and REM sleep ($p < 0.001$)(Figures 2A and 2B), while frequencies in the gamma band (30–80 Hz) were not affected.

HCN1 channel activation also affects the shape of theta waves when analyzed in the time domain. No significant difference was found in the area from the trough to the peak of the rising phase of the theta wave. However, the peak to trough area during the falling phase of the theta wave was significantly different between *HCN1*$^{-/-}$ and *HCN1*$^{+/+}$ animals during both wheel running ($p < 0.01$) and REM sleep ($p < 0.01$) (Figures 2C and 2D), indicating that the deletion of HCN1 attenuates theta wave asymmetry. Thus, HCN1 channels are not obligatory for the generation of hippocampal network rhythms in vivo, but they may affect the proper physiological expression of theta frequency activity.

Role of HCN1 in the Physiological Properties of CA1 Pyramidal Cells

Since CA1 pyramidal neurons represent spatial information, are important for learning and memory, and strongly express HCN1 in their distal dendrites, we focused our cellular analysis on the contribution of HCN1 to the integrative properties of these neurons.

Rapid and Full Activation of Pyramidal Cell I_h *Requires HCN1 Channels*

Comparison of the properties of I_h in CA1 pyramidal cells with cloned HCN channels suggests that the current is due to heteromeric channels formed by HCN1 and HCN2 subunits (Chen et al., 2001; Ulens and Tytgat, 2001). We investigated the contribution of HCN1 to I_h isolated pharmacologically at room temperature. Qualitatively similar results were obtained with standard recording conditions at 32°C–34°C (Supplemental Figures S4A and S4B). Hyperpolarizing voltage steps activated I_h in CA1 pyramidal cells from all lines of mice (Figure 3). However, deletion of HCN1 reduced the amplitude of I_h by approximately two thirds. As knockout of HCN2 reduces the amplitude of I_h by approximately one third (Ludwig et al., 2003), the sum of the residual I_h from HCN1 and HCN2 knockout mice can account for all of the wild-type current. Deletion of HCN1 also dramatically slowed the activation and deactivation kinetics of I_h. The activation timecourse of I_h from *HCN1*$^{+/+}$ or *HCN1*$^{f/f}$ mice required a sum of two exponentials for an adequate fit, whereas I_h from *HCN1*$^{-/-}$ or *HCN1*$^{f/f,cre}$ mice was generally well fit with a single exponential function (Figures 3E–3G). The slower kinetics of the residual I_h in mice with deletion of HCN1 are similar to those of cloned HCN2 channels, whereas the kinetics of I_h in HCN2 knockout mice resemble those of cloned HCN1 channels (Ludwig et al., 2003). Thus, HCN1 and HCN2 appear to be the major determinants of I_h in CA1 pyramidal cells.

HCN1 Channels Contribute to the Resting Membrane Properties of CA1 Pyramidal Cells

We investigated the contribution of HCN1 to the physiological properties of CA1 pyramidal cells using current clamp recordings in standard ACSF at 33°C–35°C (Figure 4, Supplemental Figures S4C and S4D, and Table 1). CA1 pyramidal cells from either control or knockout mice did not fire spontaneous action potentials. Deletion of HCN1 shifted the resting potential to more negative values, increased the input resistance, and prolonged the membrane time constant. Activation of I_h in response to negative current steps can drive a depolarizing membrane potential "sag" (Figures 4C and 4D). The amplitude of the sag, quantified as the ratio of the peak hyperpolarization to the steady-state hyperpolarization, was not altered by knockout of HCN1. However, when the sag was quantified as the ratio of the peak hyperpolar-

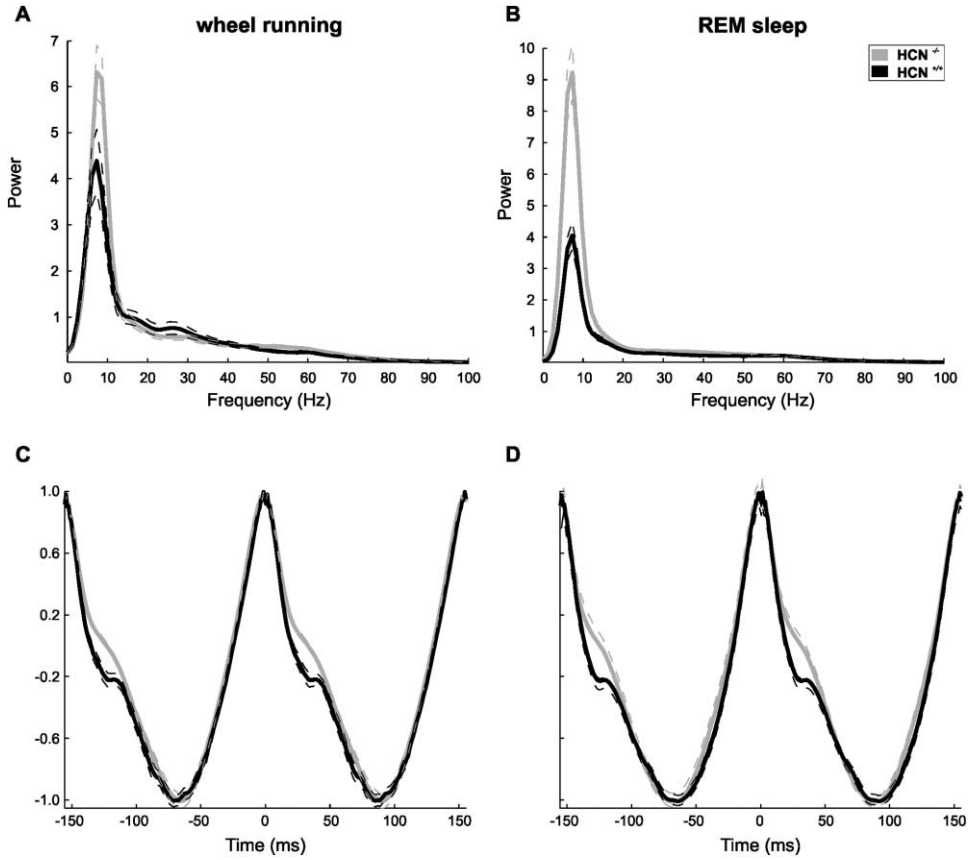

Figure 2. HCN1 Is Not Required for Hippocampal Network Rhythms but May Selectively Suppress Theta Frequency Activity

(A and B) Power spectra of hippocampal local field activity from the CA1 pyramidal layer. Group data (mean ± SEM) during wheel running and REM sleep. Note significantly larger theta power peaks ($p < 0.01$) during both behaviors.

(C and D) Peak-triggered theta wave averages (±SEM) during wheel running and REM sleep. The area between peak and trough (~0–90 ms) was significantly different between *HCN1*$^{-/-}$ and *HCN1*$^{+/+}$ mice ($p < 0.01$) during both wheel running and REM sleep.

ization to the mean hyperpolarization between 400 and 500 ms after the onset of the current step, it was reduced significantly, reflecting the slower kinetics of the residual I_h.

Responses to Low-Frequency Inputs Are Preferentially Attenuated by HCN1 Channels

Previous studies have suggested that I_h contributes to a resonant peak in the voltage response of pyramidal neurons to oscillatory current inputs at around theta frequencies (Hu et al., 2002; Pike et al., 2000). Since this appears at odds with the enhanced theta power seen upon deletion of HCN1, we determined the response of CA1 pyramidal cells to injection of oscillating currents of linearly increasing frequency (Strohmann et al., 1994). In CA1 pyramidal cells from *HCN1*$^{f/f}$ mice, the amplitude of the membrane potential oscillation appeared constant or increased slightly up to frequencies of approximately 4–8 Hz and then decayed steeply (Figure 5A). By contrast, the amplitude of the membrane potential response of CA1 pyramidal cells from *HCN1*$^{f/f,cre}$ mice was larger than that of HCN1$^{f/f}$ mice at low frequencies but not at higher frequencies (Figure 5B).

The relationship between membrane impedance and input frequency, obtained from the voltage responses (see Experimental Procedures), clearly shows that HCN1 channels preferentially attenuate responses to low-frequency inputs (Figure 5C and Supplemental Figure S5), indicating that I_h contributes to resonance by reducing membrane impedance at frequencies below the theta range. Similar effects of HCN1 on the frequency-impedance relationships of CA1 pyramidal cells were found in a comparison of *HCN1*$^{+/+}$ and *HCN1*$^{-/-}$ mice (data not shown). Thus, deletion of HCN1 causes a general enhancement in the voltage response to low-frequency oscillatory currents, consistent with the enhancement in theta power.

Properties of Schaffer Collateral and Perforant Path Inputs to CA1 Pyramidal Cells

Given the important role of HCN1 in determining the subthreshold properties of CA1 neurons, we next examined the effect of HCN1 deletion on synaptic responses to activation of the two major excitatory inputs to CA1 neurons: the direct cortical input via the perforant path and the hippocampal input from the Schaffer collateral pathway (Figure 6). For Schaffer collateral inputs, the relationship between somatic excitatory postsynaptic potential (EPSP) slope and stimulus strength was similar for *HCN1*$^{f/f,cre}$ compared with *HCN1*$^{f/f}$ mice, indicating that HCN1 has little influence on the amplitude of the postsynaptic response to a single presynaptic stimulus.

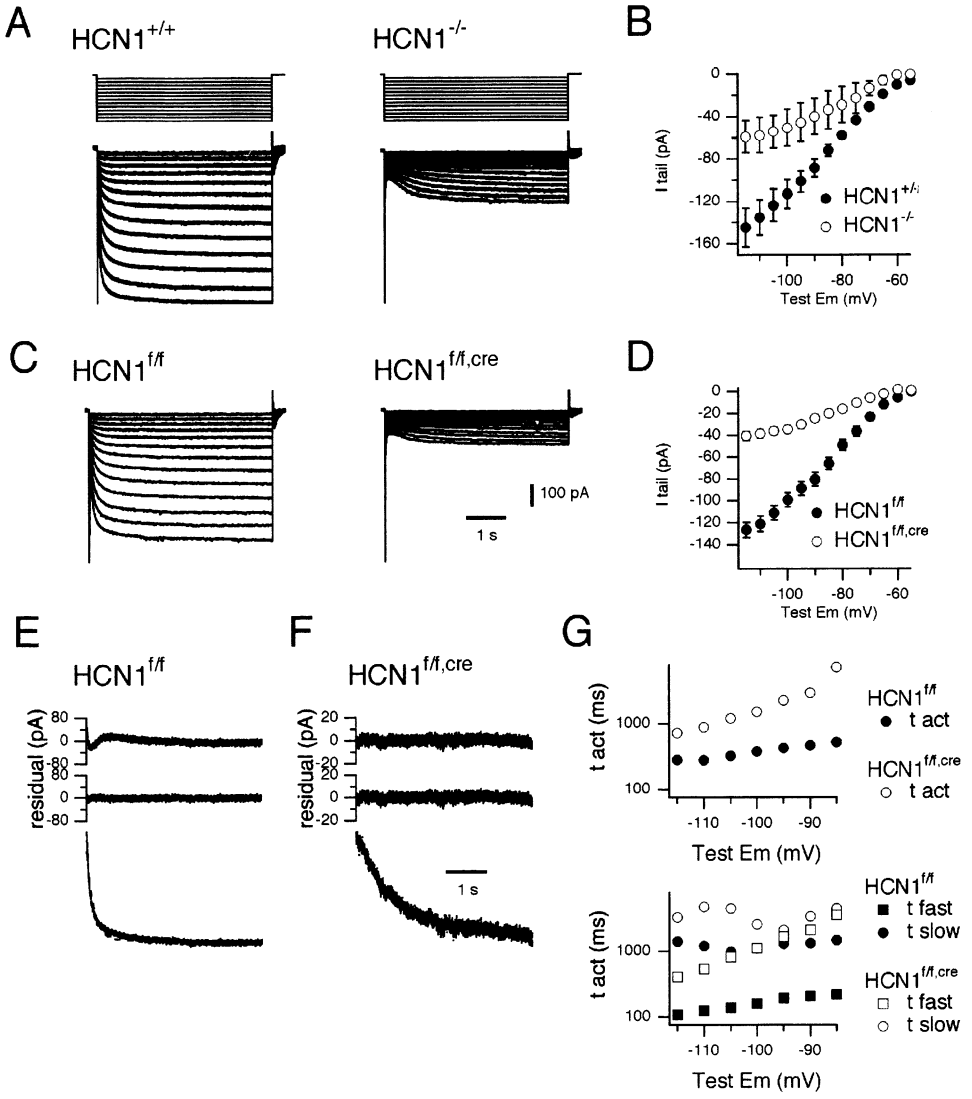

Figure 3. HCN1 Is Required for Rapid and Full Activation of I_h in CA1 Pyramidal Cells

(A) Examples of membrane currents (bottom) from *HCN1*$^{+/+}$ (left) and *HCN1*$^{-/-}$ (right) mice, evoked by hyperpolarizing voltage steps (top). Voltage steps have duration 5 s and are from a holding potential of −50 mV to potentials down to −115 mV in 5 mV increments.

(B) Mean amplitude of I_h tail currents plotted against test potential. I_h from *HCN1*$^{-/-}$ mice is reduced to approximately 40% of that in *HCN1*$^{+/+}$ mice (tail currents following steps to −115 mV: *HCN1*$^{+/+}$ −144.7 ± 18.4 pA, n = 4; *HCN1*$^{-/-}$ −59.1 ± 15.4 pA, n = 5; p = 0.009).

(C and D) Membrane currents evoked by hyperpolarizing voltage steps as in (A) and mean tail currents as in (B), except data are from *HCN1*$^{f/f}$ (n = 6) and *HCN1*$^{f/f,cre}$ mice (n = 6). Deletion of HCN1 reduces I_h to approximately 30% of its control amplitude (tail current amplitudes following steps to −115 mV: *HCN1*$^{f/f}$ −126.6 ± 7.1; *HCN1*$^{f/f,cre}$ −40.6 ± 3.9; p = 0.003). In (B) and (D) the shallow slope of the I-V relationship is probably due to poor space clamp of currents originating from distal dendritic regions.

(E and F) Activation of current responses to steps from −50 mV to −110 mV (bottom traces), from *HCN1*$^{f/f}$ and (E) and *HCN1*$^{f/f,cre}$ mice (F). The residuals obtained from fitting the current activation with a single exponential (top) or with the sum of two exponentials (middle) are also shown.

(G) Mean time constants obtained from fitting the activation of I_h with a single exponential (top) or the sum of two exponentials (bottom) are plotted against the test membrane potential. Deletion of HCN1 caused an approximately 2.5-fold slowing of the activation time constant (tact) obtained by fitting with a single exponential (activation time constants at −115 mV: *HCN1*$^{f/f}$ 282.3 ± 10.5 ms; *HCN1*$^{f/f,cre}$ 725.4 ± 9.7 ms; p = 2.6e-05). The time constants for deactivation (tdeact) of I_h were also slowed by deletion of HCN1 (for steps from −115 mV to −50 mV, tdeact = 138.3 ± 5.8 ms for *HCN1*$^{f/f}$ versus 319.5 ± 9.0 ms for *HCN1*$^{f/f,cre}$, p = 0.003).

However, the area of subthreshold Schaffer collateral EPSPs was increased in pyramidal cells from *HCN1*$^{f/f,cre}$ mice, indicating that HCN1 channels do modulate the decay of Schaffer collateral EPSPs. By contrast, both the amplitude and area of somatically recorded perforant path EPSPs was increased in *HCN1*$^{f/f,cre}$ mice (Figures 6D and 6E). In addition, perforant path EPSPs had slower rise times and decay kinetics in cells from *HCN1*$^{f/f,cre}$ compared with *HCN1*$^{f/f}$ mice. This difference in EPSP kinetics was larger for perforant path compared to Schaffer collateral EPSPs, suggesting that the higher expression of HCN1 channels in the distal dendrites of CA1 pyramidal cells enables them to exert a greater influence on integration of distal synaptic inputs. We

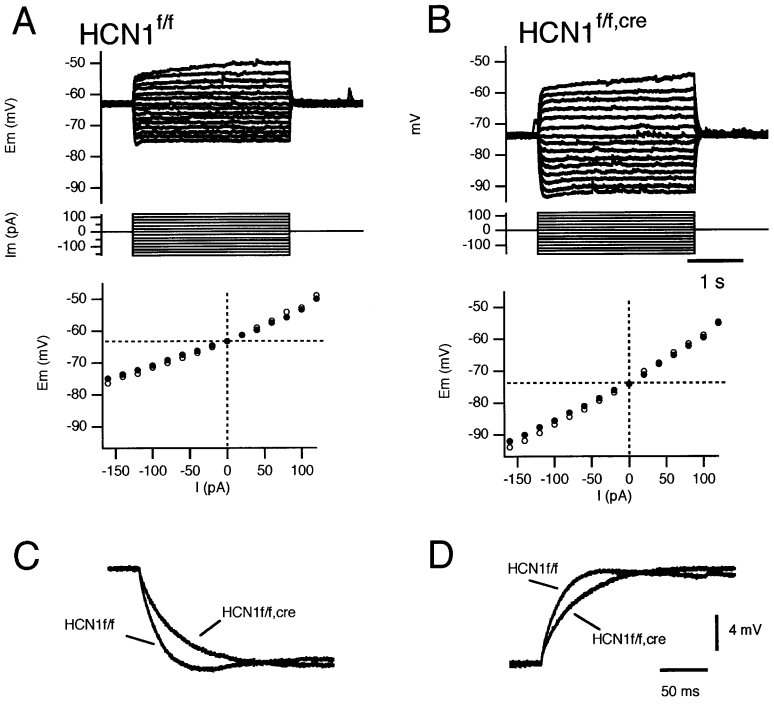

Figure 4. HCN1 Influences the Subthreshold Membrane Properties of CA1 Pyramidal Cells

(A and B) Examples of membrane potential responses (top) of CA1 pyramidal cells from a *HCN1*$^{f/f}$ (A) and a *HCN1*$^{f/f,cre}$ mouse (B) to a series of current steps (middle). The peak hyperpolarization (open symbols) and steady-state membrane potential (closed symbols) are plotted as a function of the current step amplitude (bottom). Dotted lines indicate the resting membrane potential.

(C and D) Comparison of the onset (C) and offset (D) of similar amplitude responses to currents steps demonstrates the faster membrane time constant of pyramidal cells from *HCN1*$^{f/f}$ compared with *HCN1*$^{f/f,cre}$ mice. Note the membrane potential "sag" following the peak hyperpolarization of the *HCN1*$^{f/f}$ response. Records are from the data shown in (A) and (B).

did not find any difference between the two groups of mice in the relationship between stimulus intensity and the slope of extracellular field EPSPs in either pathway, indicating that deletion of HCN1 does not alter basal transmitter release or the excitatory postsynaptic current (Figures 6F–6G and Supplemental Figure S6).

HCN1 Channels Preferentially Attenuate LTP at Distal Perforant Path Synapses and Not Proximal Schaffer Collateral Synapses

Could changes in dendritic integration caused by deletion of HCN1 alter the induction of synaptic plasticity? We compared the effect of HCN1 deletion on LTP of Schaffer collateral and perforant path inputs to CA1 (Figure 7). We found no difference between *HCN1*$^{f/f}$ and *HCN1*$^{f/f,cre}$ mice in the magnitude of LTP in the Schaffer collateral pathway induced by a theta-burst protocol or with a number of other standard LTP protocols and recording conditions (Supplemental Figure S6). The absence of any effect of HCN1 on LTP of Schaffer collateral inputs is also consistent with previous pharmacological studies (Wang et al., 2003). In contrast to the Schaffer collateral pathway, the amplitude of LTP at synapses in the perforant path was dramatically enhanced in slices from *HCN1*$^{f/f,cre}$ mice compared with *HCN1*$^{f/f}$ mice. Thus, the high density of HCN1 channels found in the distal dendrites of CA1 pyramidal cells, which receive the perforant path synaptic inputs, appears to act as an inhibitory constraint on the induction of LTP in this pathway. By contrast, HCN1 channels have a relatively low density in the proximal apical dendrites and do not appear to influence LTP at Schaffer collateral inputs, which synapse onto this part of the apical dendritic tree.

Discussion

Our behavioral and electrophysiological experiments, using mice with general and forebrain-restricted deletion of HCN1 channels, provide evidence that dendritic integration by forebrain pyramidal neurons can constrain both learning and memory as well as synaptic plasticity. We suggest that HCN1 channels in the distal dendrites of pyramidal cells could act as inhibitory con-

Table 1. Comparison of the Membrane Properties of CA1 Pyramidal Cells from *HCN1*$^{f/f}$ and *HCN1*$^{f/f,cre}$ Mice

	HCN1$^{f/f}$		HCN1$^{f/f,cre}$		
	Mean ± SEM	n	Mean ± SEM	n	p
Em (mV)	−68.0 ± 0.9	21	−73.6 ± 0.7	23	6.1e-06
IR −ve (MΩ)	100.0 ± 7.5	21	138.0 ± 12.6	23	0.012
IR +ve (MΩ)	116.0 ± 9.1	21	161.5 ± 13.6	23	0.008
Tm (ms)	22.0 ± 1.65	21	33.2 ± 3.6	21	0.003
Sag (ss)	0.88 ± 0.01	21	0.86 ± 0.01	23	0.892
Sag (early)	0.88 ± 0.01	21	0.92 ± 0.01	23	0.022

Resting membrane potential (Em), input resistance measured from responses to negative current steps (IR −ve), input resistance measured from responses to positive current steps (IR +ve), estimated membrane time constant (Tm), and the size of the membrane potential sag during a negative current step (sag ratio), measured either at steady-state (ss) or from the mean membrane potential between 400 and 500 ms after the onset of the current step (early).

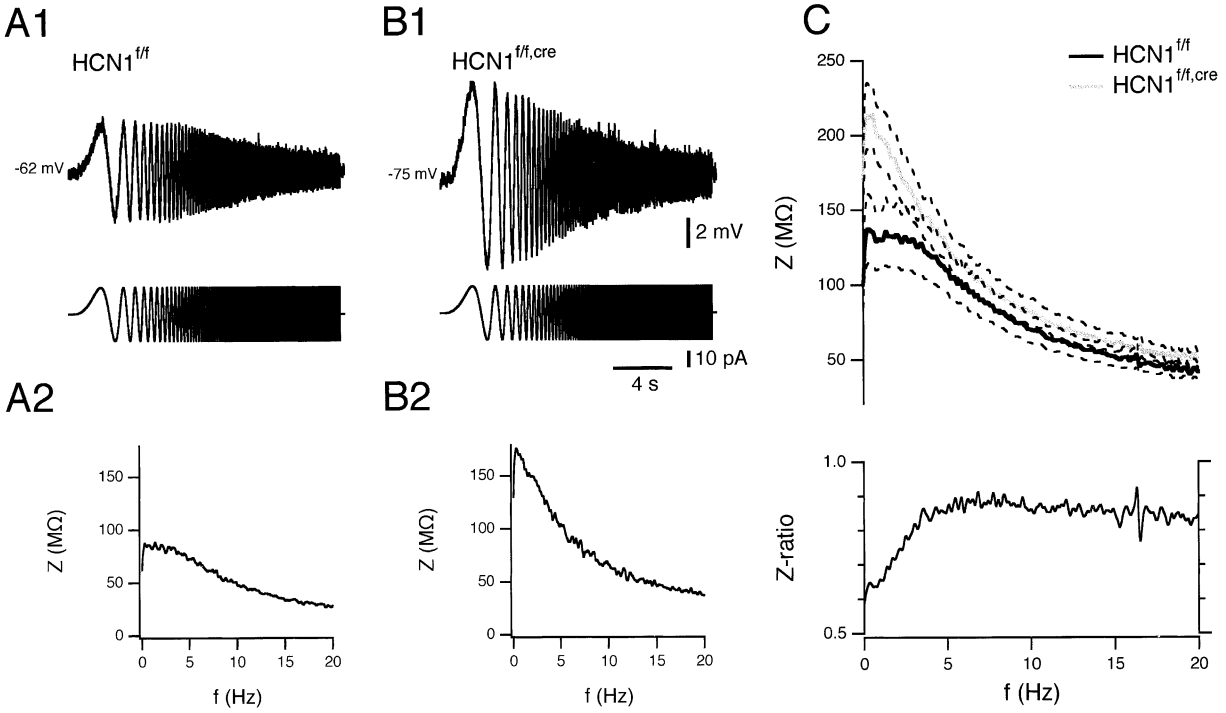

Figure 5. HCN1 Preferentially Attenuates Responses of CA1 Pyramidal Cells to Low-Frequency Inputs

(A and B) The frequency-response properties of CA1 pyramidal cells from *HCN1$^{f/f}$* (A) and *HCN1$^{f/f,cre}$* mice (B) characterized by analysis of membrane potential responses to oscillating current inputs.

(A1 and B1) Examples of membrane potential responses (top) to oscillating current inputs (bottom).

(A2 and B2) Plot of membrane impedance as a function of input frequency calculated from the data in (A1) and (B1).

(C) Mean impedance magnitude (Z) and ratio of impedance magnitude in *HCN1$^{f/f}$* to that in *HCN1$^{f/f,cre}$* mice (Z ratio) plotted as a function of input frequency. Dashed lines indicate standard error of the mean. At frequencies $<$1.6 Hz the impedance of pyramidal cells from *HCN1$^{f/f,cre}$* mice ($n = 10$) is significantly ($p < 0.05$) higher than HCN1$^{f/f}$ controls ($n = 10$). The preferential attenuation of low-frequency inputs by HCN1 channels is illustrated by the much smaller z ratio for input frequencies less than 2 Hz compared with input frequencies above 5 Hz.

straints on learning by damping postsynaptic changes in membrane potential that at distal dendrites might otherwise trigger synaptic plasticity.

HCN1 Channels Constrain Short- and Long-Term Memory

Several previous studies have found an enhancement in performance of learning and memory tasks using genetic modifications that either downregulate intracellular signaling pathways that constrain synaptic plasticity, overexpress molecules involved in the expression of synaptic plasticity, or modify the properties of receptors involved in the induction of synaptic plasticity (Abel et al., 1998; Malleret et al., 2001; Routtenberg et al., 2000; Tang et al., 1999). Other genetic modifications that increase synaptic plasticity cause impairments in memory performance, indicating that the relationship between the two phenomena is complex and unpredictable (Sanes and Lichtman, 1999). So far genetic deletion of other neuronal voltage-gated ion channels has been found to impair performance of various forms of learning and memory (Kubota et al., 2001; Meiri et al., 1997; Nolan et al., 2003). By contrast, the performance of *HCN1$^{f/f,cre}$* mice was enhanced in specific components of behavioral tasks involving spatial reference memory. Together with the finding that *HCN1$^{-/-}$* mice have a profound motor learning deficit (Nolan et al., 2003), these data provide clear evidence that the same channel can have distinct functional roles in different forms of learning depending on the cellular context and neuronal circuitry in which the channel participates.

HCN1 Channels Constrain LTP at Perforant Path Synapses by Influencing the Integrative Properties of Pyramidal Neurons

We find that HCN1 channels strongly influence the integrative properties of CA1 pyramidal cells. They act as a temporal filter that preferentially attenuates low-frequency components of input waveforms and as a spatial filter that preferentially dampens distal inputs. Thus, HCN1 channels open at the resting membrane potential shunt synaptic inputs, and voltage-dependent gating of HCN1 channels further opposes membrane responses. The greater effect of HCN1 deletion on perforant path compared with Schaffer collateral inputs can be explained by the preferential distribution of HCN1 channels to distal dendrites (Lorincz et al., 2002), supporting a preferential role for the channel in integration of distal dendritic inputs (Magee, 1998). As pyramidal cells in the subiculum and in layer V of the neocortex have a dendritic distribution of I_h and HCN1 subunits similar to CA1 pyramidal neurons, HCN1 channels may have similar functions in these neurons (Berger et al., 2001; Lorincz et al., 2002; Williams and Stuart, 2000).

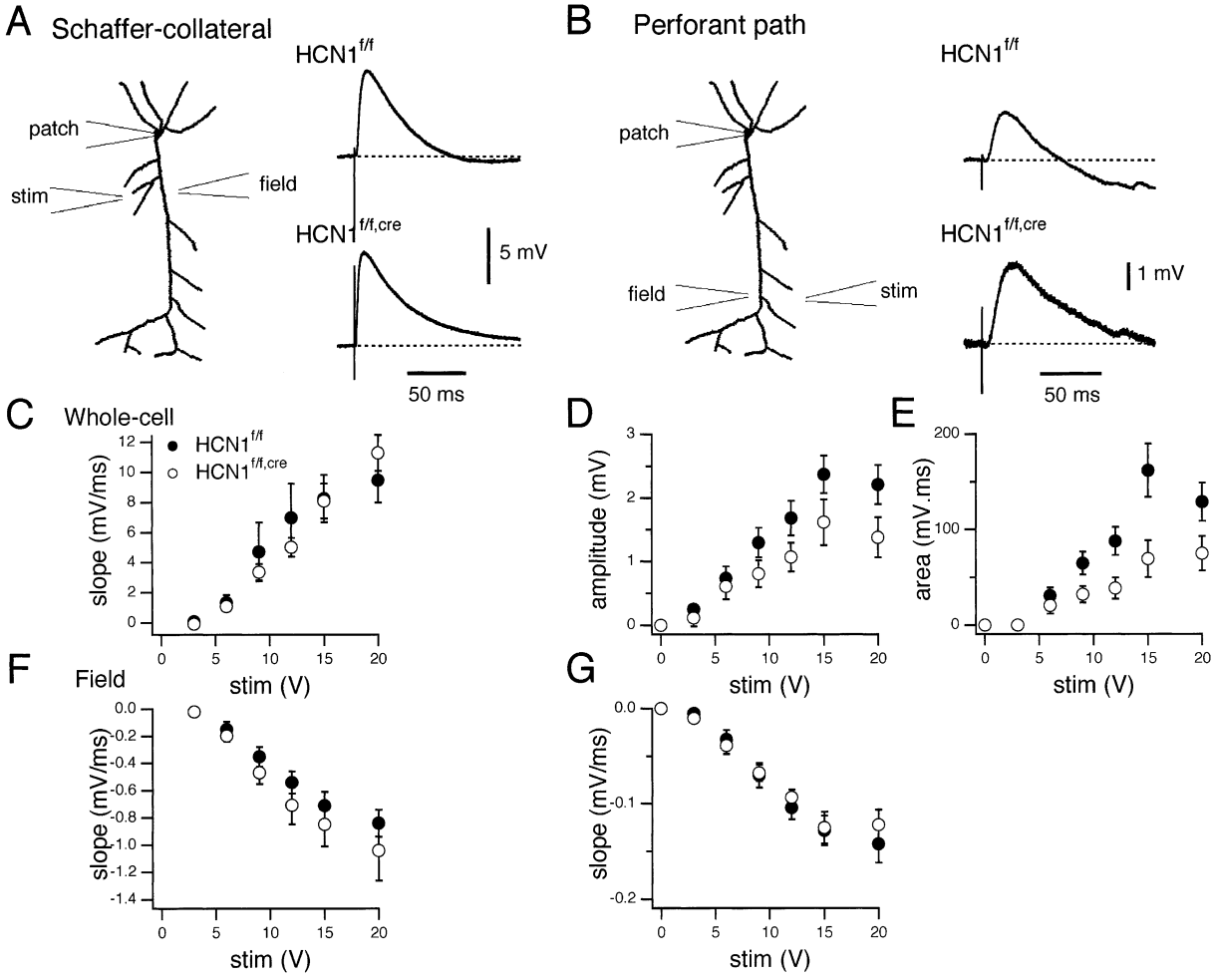

Figure 6. Effects of HCN1 Knockout on Schaffer Collateral and Perforant Path EPSPs in CA1 Pyramidal Cells

(A and B) Schematic illustration of the recording configuration and examples of somatically recorded EPSPs evoked by stimulation of Schaffer collateral inputs (A) and perforant path inputs (B). Subthreshold Schaffer collateral EPSPs from *HCN1*$^{f/f}$ mice (n = 8) and *HCN1*$^{f/f,cre}$ mice (n = 10) had 10%–90% rise times of 6.3 ± 0.9 ms and 6.7 ± 1.6 ms, respectively (p = 0.84), decay times of 38.6 ± 7.0 ms and 51.3 ± 4.8 ms (p = 0.14), and areas of 366.2 ± 55.9 mV.ms and 617.2 ± 74.6 mV.ms (p = 0.02). The mean amplitude for *HCN1*$^{f/f}$ and *HCN1*$^{f/f,cre}$ Schaffer collateral EPSPs respectively, was 10.6 ± 1.6 mV and 11.5 ± 1.7 mV (p = 0.7) with a stimulus of duration of 0.1 ms and intensity of 6 ± 0.8 V and 5.7 ± 0.5 V (p = 0.75). Subthreshold perforant path EPSPs from HCN1$^{f/f}$ mice (n = 8) and HCN1$^{f/f,cre}$ mice (n = 12) evoked by stimuli of amplitude 15 V and duration 0.1 ms had 10%–90% rise times of 7.14 ± 0.52 ms and 8.82 ± 0.80 ms, respectively (p = 0.14), halfwidths of 38.8 ± 6.4 ms and 57.6 ± 4.6 ms (p = 0.03). The mean amplitude for HCN1$^{f/f}$ and HCN1$^{f/f,cre}$ perforant path EPSPs, respectively, was 1.6 ± 0.4 mV and 2.4 ± 0.3 mV (p = 0.1) in response to stimuli with amplitude of 15 V and 1.7 ± 0.5 mV and 3.59 ± 0.6 mV (p = 0.04) in response to stimuli with amplitude of 25 V.

(C) Plot of the relationship between stimulus strength and the slope of EPSPs in CA1 pyramidal cells, from *HCN1*$^{f/f}$ mice (n = 6) and *HCN1*$^{f/f,cre}$ mice (n = 8), evoked by stimulation of Schaffer collateral inputs.

(D and E) Plot of the amplitude (D) and the area (E) as a function of stimulus strength for perforant path EPSPs recorded from CA1 pyramidal cells.

(F and G) Plot of relationship between stimulus strength and the slope of field EPSPs recorded from stratum radiatum (F) (*HCN1*$^{f/f}$, n = 10, *HCN1*$^{f/f,cre}$, n = 16) or stratum lacunosum moleculare (G) (*HCN1*$^{f/f}$, n = 8, *HCN1*$^{f/f,cre}$, n = 11) in response to activation of Schaffer collateral or perforant path inputs, respectively.

Can the absence of HCN1 channels from distal dendrites of CA1 pyramidal cells account for the enhanced perforant path LTP or the modified theta field activity? The modified integrative properties of CA1 pyramidal cells may lead to a larger postsynaptic response that enhances the induction of perforant path LTP and increases the size of theta oscillations. One potential mechanism is provided by the findings that the NMDA component of perforant path input is substantially larger than that of Schaffer collateral input and is opposed by I_h (Otmakhova and Lisman, 2004; Otmakhova et al., 2002). Thus, the removal of HCN1 channels may enhance theta-related depolarization and promote the induction of LTP by allowing increased activation of distal NMDA receptors at perforant path synapses. Deletion of HCN1 may also preferentially enhance the firing of local dendritic Ca^{2+} spikes, which are of particular importance for intrinsic theta oscillations and for induction of LTP at distal synapses on CA1 pyramidal neurons (Golding et al., 2002; Kamondi et al., 1998).

We found no evidence for any role of HCN1 in basal synaptic transmission, and ultrastructural studies have

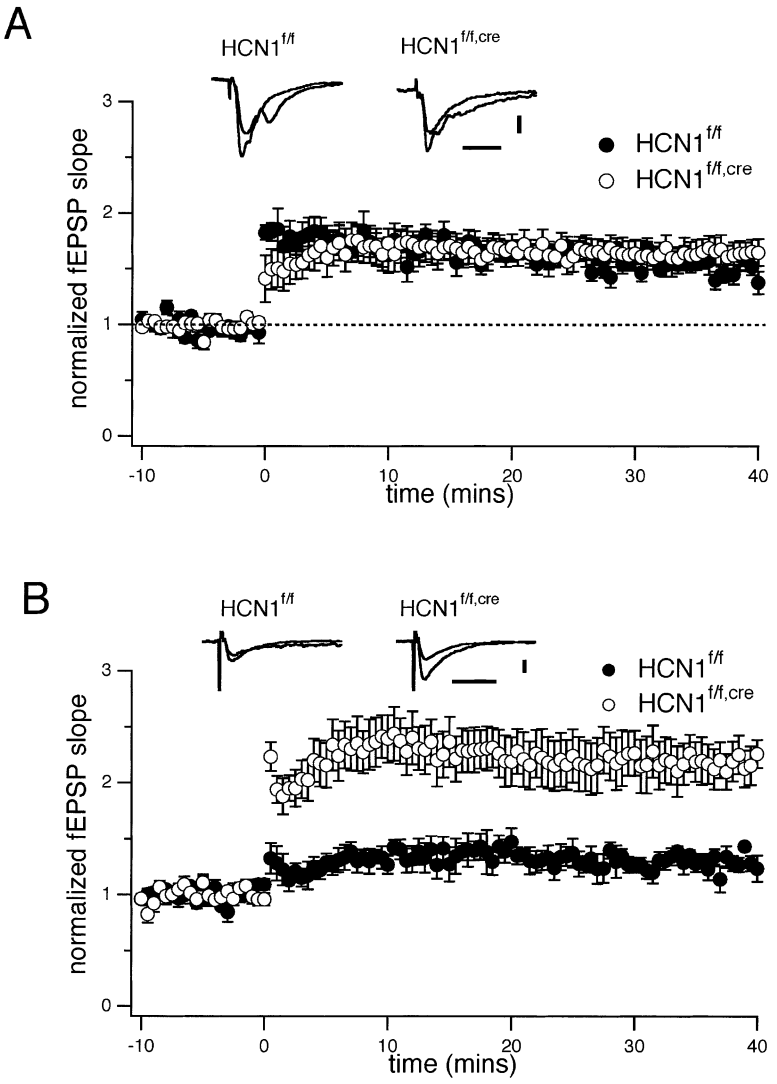

Figure 7. HCN1 Constrains LTP at Perforant Path, but Not Schaffer Collateral Inputs to CA1 Pyramidal Cells

(A and B) The mean slope of Schaffer collateral (A) (*HCN1*$^{f/f}$, n = 7, *HCN1*$^{f/f,cre}$, n = 9) and perforant path (B) (*HCN1*$^{f/f}$, n = 7, *HCN1*$^{f/f,cre}$, n = 11) fEPSPs normalized to the average baseline slope is plotted as a function of time. LTP is induced at time zero. Insets show representative field EPSPs from *HCN1*$^{f/f}$ and *HCN1*$^{f/f,cre}$ mice. Scale bars in (A) are 10 ms and 0.5 mV and in (B) are 20 ms and 0.2 mV. There was a significant difference between *HCN1*$^{f/f}$ and *HCN1*$^{f/f,cre}$ mice in the amplitude of LTP 40 min after induction at perforant path ($p = 0.001$), but not Schaffer collateral inputs ($p > 0.05$).

localized HCN1 to postsynaptic dendrites, but not presynaptic axonal inputs to CA1 or subicular pyramidal neurons (Lorincz et al., 2002; Notomi and Shigemoto, 2004), supporting a postsynaptic integrative role of HCN1 in modulation of perforant path inputs. Although HCN1 is expressed in some inhibitory interneurons, their contribution to the enhanced LTP can be ruled out since the LTP experiments were performed in the presence of $GABA_A$ and $GABA_B$ blockers. Although the perforant path input to CA1 is the single most important contributor to the extracellular theta field in the hippocampus (Buzsaki, 2002), actions of HCN1 channels in interneurons in these in vivo experiments cannot be ruled out. However, it is unlikely that the modified theta is due to the loss of HCN1 from septal neurons, which provide an input to the hippocampus that is important for theta rhythm generation, as HCN1 expression levels in the medial septum are low (Santoro et al., 2000) and blockade of I_h in this region reduces the frequency and attenuates, rather than increases, the power of hippocampal theta activity (Xu et al., 2004).

Selective Control of Plasticity at Perforant Path Inputs to the Distal Dendrites of CA1 Pyramidal Cells: A Possible Mechanism for the Influence of HCN1 Channels on Learning and Memory

How might deletion of HCN1 from CA1 pyramidal cells enhance performance of learning and memory tasks? The hippocampal trisynaptic circuit, from layer II of the entorhinal cortex via the dentate gyrus to CA3 and then to CA1, has been thought of as the major pathway for the relay of information from the associational areas of the neocortex through the hippocampus (Anderson et al., 1971). However, synaptic plasticity in the trisynaptic circuit may not be required for some forms of hippocampal-dependent learning and memory. Rather inputs from layer III of the entorhinal cortex to neurons in CA1 may also be of functional importance (Figure 8) (Brun et al., 2002; Huang et al., 1995; Witter et al., 2000). Our study shows that synaptic plasticity at these direct entorhinal inputs, but not at the more proximal Schaffer collateral inputs, is strongly regulated by HCN1 channels. Thus, the enhanced performance in spatial learning and mem-

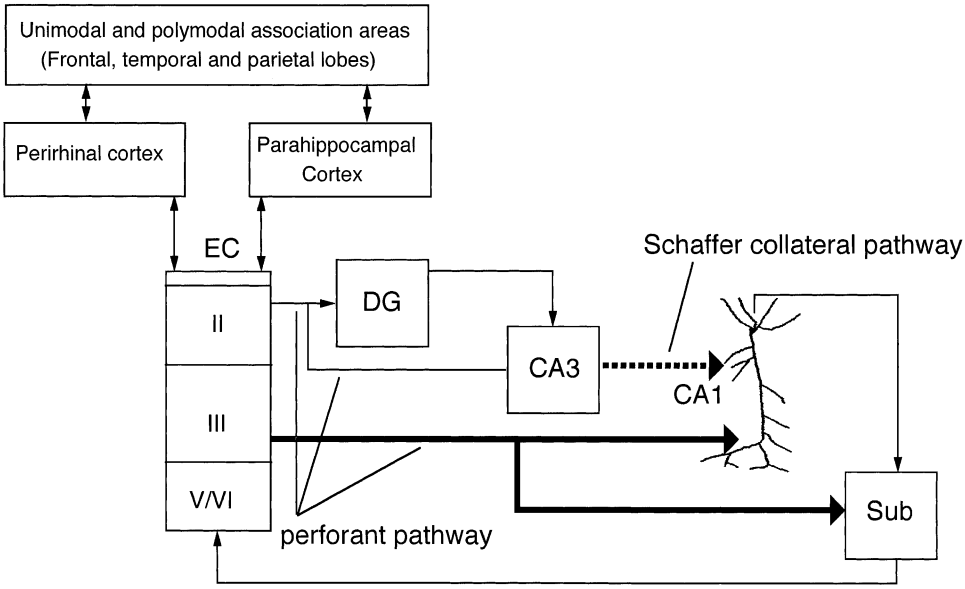

Figure 8. The Organization of Medial Temporal Lobe Circuits

Information flows through the hippocampal trisynaptic circuit from layer II of the entorhinal cortex (EC) via the dentate gyrus (DG) to CA3 and then to CA1. The input from CA3 to CA1, via the Schaffer collateral pathway, targets the proximal dendrites of CA1 pyramidal neurons and is indicated by the dashed line. In addition, CA1 neurons receive a direct input from the EC to their distal apical dendrites via the perforant path indicated by the bold line. The distal apical dendrites of CA1 pyramidal neurons contain the highest density of HCN1 channels. This figure was modified from Huang et al., 1995.

ory tasks in the *HCN1*$^{f/f,cre}$ mice may reflect the removal of the inhibitory constraint on LTP at the perforant path inputs to CA1 neurons. It has been suggested that CA1 pyramidal neurons compare sensory information provided via the direct cortical perforant path inputs with predictions made by the dentate/CA3 region on the basis of previously stored information (Lisman, 1999). Increased LTP of perforant path inputs in the absence of HCN1 may, thus, facilitate recall when stored associations from CA3 match information about a familiar environment provided by the perforant path input to CA1.

Because HCN1 was deleted throughout the forebrain, we cannot definitively assign the behavioral phenotype to any one cell type. In addition to CA1 pyramidal neurons, HCN1 is also strongly expressed in pyramidal neurons in the subiculum, the postsynaptic target of the CA1 pyramidal neurons, and in neocortical layer V pyramidal neurons. Since HCN1 also shows its characteristic gradient of increasing expression in the apical dendrites of these pyramidal cells, deletion of HCN1 may also enhance plasticity at their distal synaptic inputs. Moreover, the present data do not rule out a contribution of HCN1 in nonpyramidal neurons, for example entorhinal stellate cells, to the behavioral phenotype. Further spatial restriction of the HCN1 deletion will be required to distinguish these possibilities.

In summary, our findings suggest that learning and memory is constrained by the spatial and temporal integrative properties of neuronal dendrites. The ability to enhance the performance of a behavior by deleting an ion channel is surprising and leads to the question of what evolutionary advantageous function the channel may perform. HCN1 channels may maximize the information capacity of pyramidal cells by normalizing the somatic waveform of synaptic inputs so that temporal summation of EPSPs becomes independent of their synaptic location (Magee, 1999). Neuromodulators that gate the ability to store information during different behavioral states may shift the relative importance of proximal versus distal synaptic inputs by modulating HCN1 channel activity. Both possibilities are compatible with our findings as the demands placed on forebrain neurons during the behavioral tasks that we have used may be well below the maximum capacity to which they have evolved. Thus, the dendritic mechanisms for normalization or modulation of synaptic inputs may have evolved at a modest cost to the ability to modify the strength of synaptic connections.

Experimental Procedures

The generation of the lines of mice used in this study has been described previously (Nolan et al., 2003). *HCN1*$^{f/f,cre}$ and *HCN1*$^{f/f}$ littermates with mixed average 50/50% 129SVEV/C57 background were used in experiments. Mice were maintained and bred under standard conditions, consistent with National Institutes of Health guidelines and approved by the Institutional Animal Care and Use Committee. Mean values are stated as ± standard error of the mean (SEM). On figures in which error bars are absent the SEM is smaller than the symbol size.

Behavior

For all behavioral tasks, mutant and control littermates (males, 3 months old) were used. Statistical analyses used ANOVAs with genotype as the between-subject factor. The experimenter was blind to the genotype in all studies.

The water maze task was performed as previously described (Malleret et al., 1999) with three training phases: 2 days with a visible platform followed by 4 days with a hidden platform in quadrant

number 3, followed by 8 days with the hidden platform in quadrant number 1. For the first two phases, four trials, 120 s maximum duration and 15-min intertrial interval, were given daily. For the third phase, only one trial was given each day. In the first experiment, 15 min before the first trial of each phase, the mice were primed by allowing them to rest on the platform for 15 s. The second experiment used a new group of mice and the same experimental paradigm, expect that the priming procedure was omitted. Probe trials, during which the platform was removed from the maze, lasted 60 s. The trajectories of mice in the maze were recorded with a video tracking system (HVS Image Analysis System VP-118).

In Vivo Electrophysiology

Male *HCN1*$^{-/-}$ (n = 9) and *HCN1*$^{+/+}$ (n = 6) mice were implanted with chronic recording tetrodes (four 12-μm polyimide-coated nichrome wires) or 60-μm wires under anesthesia (Buhl et al., 2003). The electrodes were gradually moved to the CA1 pyramidal layer. The position of the electrode in the CA1 pyramidal layer was determined by the presence of fast oscillations ("ripples") in association with synchronous discharge of neurons (Buzsáki et al., 2003). Once in the layer, maximum ripple amplitudes were used as an online reference for consistent electrode placement between animals.

Electrical activity was recorded from each animal during slow wave sleep (SWS) and rapid eye movement sleep (REM) in its home cage and during the wake cycle while the animal was running in a wheel. The mice were allowed to freely explore the apparatus which consisted of a running wheel (29.5 cm in diameter) and adjacent box (30 cm × 40 cm × 35 cm; Czurko et al., 1999). Field potential and unit activity were recorded after being amplified (2000×) and band-pass filtered (1–5 kHz; model 12-64 channel; Grass Instruments, Quincy, Massachusetts), digitized with 14-bit resolution continuously at 20 kHz, and recorded on a PC using custom Labview software (National Instruments, Austin, Texas). Running speed of the mouse was measured from the output of an optical encoder attached to the wheel. The data were analyzed offline. When bilateral recordings were made, recordings from each hemisphere were treated as independent data.

The beginning, middle, and end of CA1 ripple events were detected by applying an amplitude threshold (mean +7 SD) to the previously bandpass-filtered (150–250 Hz) EEG. Theta and gamma epochs, amplitudes, and phases were detected by applying a Hilbert transform to the previously bandpass-filtered (4–12 Hz and 30–80 Hz, respectively) EEG (Buhl et al., 2003). The mean gamma amplitude was then calculated for every 10° of the theta cycle. All comparisons of ripples, theta, and gamma events were taken from the same electrode location in the CA1 pyramidal layer. At the end of the experiment, the animal was perfused and the location of the electrode tips were histologically verified (Buhl et al., 2003). Differences between groups were compared with an unpaired Student's t test.

In Vitro Electrophysiololgy

Horizontal brain slices were prepared from 4- to 10-week-old mice. Mice were decapitated, their brains rapidly removed and placed in cold (2°C −4°C) modified ACSF of composition (mM) NaCl (86), NaH_2PO_4 (1.2), KCl (2.5), $NaHCO_3$ (25), Glucose (25), $CaCl_2$(0.5), $MgCl_2$(7), sucrose (75). The hemisected brain was glued to an agar block and cut submerged under cold modified ACSF into 400 μm sections with a Vibratome 3000 sectioning system. Slices were transferred to a storage container filled with standard ACSF at 33°C −35°C for 20–30 min and then allowed to cool to room temperature (20°C −22°C). The standard ACSF had the following composition (mM): NaCl (124), NaH_2PO_4 (1.2), KCl (2.5), $NaHCO_3$ (25), Glucose (20), $CaCl_2$ (2), $MgCl_2$ (1). The modified ACSF for isolation of I_h had the following composition (mM): NaCl (115), NaH_2PO4 (1.2), KCl (5), NaHCO3 (25), glucose (20), CaCl2 (2), MgCl2 (1), BaCl2 (1), CdCl2 (0.1), 4-AP (1), TEA (5), NBQX (0.005), bicuculline (0.02), and TTX (0.0005). For recording, slices were transferred to a submerged chamber at room temperature for isolation of I_h and at 33°C −35°C for all other experiments. Whole-cell recordings were obtained from CA1 pyramidal cell bodies, visually identified under infrared illumination with DIC optics, using 2–5 MΩ resistance electrodes filled with intracellular solution of composition (mM): KMethylsulfate (120), KCl (20), HEPES (10), $MgCl_2$(2), EGTA (0.1), Na_2ATP (4), Na_2GTP (0.3), phosphocreatine (10). Series resistances were ≤15 MΩ for voltage-clamp experiments and ≤40 MΩ for current-clamp experiments. There was no significant difference between the series resistance of recordings between experimental groups in either configuration. Series resistance in voltage-clamp recordings was compensated by 50%–80%. For current-clamp recordings appropriate bridge and electrode capacitance compensation were applied. Membrane current and voltage were filtered at 1–2 KHz and 4–20 KHz and sampled at 5–10 KHz and 10–50 KHz for voltage- and current-clamp experiments, respectively.

Glutamatergic EPSPs were investigated in the presence of either bicuculline or picrotoxin and CGP55845 to block $GABA_A$ and $GABA_B$ receptors, respectively. CA3 was removed from the slice to prevent emergence of epileptiform discharges after blocking GABA receptors. A concentric bipolar stimulating electrode was placed in stratum radiatum to evoke Schaffer collateral inputs or stratum lacunosum molecularae to evoke perforant path inputs. A patch electrode containing ACSF was placed in the same layer as the stimulating electrode at a distance of 100–200 μm to record the corresponding field EPSP. Selective activation of perforant path axons was confirmed by observation of a reversal in the polarity of the field EPSP when it was recorded from stratum radiatum (Colbert and Levy, 1993). Synaptic responses to various intensities of stimulation (3–20 V, 0.1 ms) were recorded locally with field electrodes and in the whole-cell configuration from the soma of individual CA1 pyramidal cells. The stimulus strength was then set to give a field EPSP with slope approximately 50% of the maximum. A 10–15 min baseline was obtained before giving four theta-burst trains of stimuli at 20 s intervals. Each theta-burst train consisted of five bursts at a frequency of 5 Hz with each burst containing 10 stimuli at a frequency of 100 Hz. Synaptic responses were then recorded for a further 40 min and in most cases for >60 min. Protocols used for additional LTP experiments are described in Supplemental Figure S6 on the *Cell* website.

Data were analyzed in IGOR pro (Wavemetrics) using custom written routines. To determine impedance-frequency relationships, membrane potential response to current inputs that oscillated with linearly increasing frequency were recorded (Strohmann et al., 1994). Membrane impedance was calculated from the ratio of the Fourier transform of membrane potential to the Fourier transform of injected current. The field EPSP slope was determined by fitting a straight line to the initial rising phase following the fiber volley. An identical time window (width 1–2 ms) was used for slope measurements of all field EPSPs from the same experiment. Statistical significance was tested with Student's t test.

Acknowledgments

We thank Sebastien Thuault and Juan Marcos Alarcon for comments on the manuscript. This work was supported by the Howard Hughes Medical Institute, The Kavli Insitute for Brain Sciences, grants from NIH to E.R.K. (MH045923), S.A.S. (NS36658), and G.B. (NS34994, MH54671), a Wellcome Trust travel fellowship (M.F.N.), a NSF Graduate Research Fellowship (J.T.D.), and the New York State Research Foundation for Mental Hygiene. E.R.K. is one of the four founders of Memory Pharmaceuticals and Chairman of its Scientific Advisory Board. Memory Pharmaceuticals is concerned with developing drugs for age-related memory loss. Some of these drugs are also potentially useful in depression and schizophrenia.

Received: June 6, 2004
Revised: August 27, 2004
Accepted: October 4, 2004
Published: November 23, 2004

References

Abel, T., Martin, K.C., Bartsch, D., and Kandel, E.R. (1998). Memory suppressor genes: inhibitory constraints on the storage of long-term memory. Science *279*, 338–341.

Anderson, P., Bliss, T.V., and Skrede, K.K. (1971). Lamellar organization of hippocampal pathways. Exp. Brain Res. *13*, 222–238.

Berger, T., Larkum, M.E., and Luscher, H.R. (2001). High I(h) channel

density in the distal apical dendrite of layer V pyramidal cells increases bidirectional attenuation of EPSPs. J. Neurophysiol. *85*, 855–868.

Bi, G.Q., and Poo, M.M. (1998). Synaptic modifications in cultured hippocampal neurons: dependence on spike timing, synaptic strength, and postsynaptic cell type. J. Neurosci. *18*, 10464–10472.

Bliss, T.V., and Collingridge, G.L. (1993). A synaptic model of memory: long-term potentiation in the hippocampus. Nature *361*, 31–39.

Bliss, T.V., Collingridge, G.L., and Morris, R.G. (2003). Introduction. Long-term potentiation and structure of the issue. Philos. Trans. R. Soc. Lond. B Biol. Sci. *358*, 607–611.

Brun, V.H., Otnass, M.K., Molden, S., Steffenach, H.A., Witter, M.P., Moser, M.B., and Moser, E.I. (2002). Place cells and place recognition maintained by direct entorhinal-hippocampal circuitry. Science *296*, 2243–2246.

Buhl, D.L., Harris, K.D., Hormuzdi, S.G., Monyer, H., and Buzsaki, G. (2003). Selective impairment of hippocampal gamma oscillations in connexin-36 knock-out mouse in vivo. J. Neurosci. *23*, 1013–1018.

Buzsáki, G. (2002). Theta oscillations in the hippocampus. Neuron *33*, 325–340.

Buzsáki, G., Buhl, D., Harris, K., Csicsvari, J., Czeh, B., and Morozov, A. (2003). Hippocampal network patterns of activity in the mouse. Neuroscience *116*, 201–211.

Chen, S., Wang, J., and Siegelbaum, S.A. (2001). Properties of hyperpolarization-activated pacemaker current defined by coassembly of HCN1 and HCN2 subunits and basal modulation by cyclic nucleotide. J. Gen. Physiol. *117*, 491–504.

Colbert, C.M., and Levy, W.B. (1993). Long-term potentiation of perforant path synapses in hippocampal CA1 in vitro. Brain Res. *606*, 87–91.

Czurko, A., Hirase, H., Csicsvari, J., and Buzsaki, G. (1999). Sustained activation of hippocampal pyramidal cells by 'space clamping' in a running wheel. Eur. J. Neurosci. *11*, 344–352.

Fisahn, A., Yamada, M., Duttaroy, A., Gan, J.W., Deng, C.X., McBain, C.J., and Wess, J. (2002). Muscarinic induction of hippocampal gamma oscillations requires coupling of the M1 receptor to two mixed cation currents. Neuron *33*, 615–624.

Gasparini, S., and DiFrancesco, D. (1997). Action of the hyperpolarization-activated current (Ih) blocker ZD 7288 in hippocampal CA1 neurons. Pflugers Arch. *435*, 99–106.

Golding, N.L., Staff, N.P., and Spruston, N. (2002). Dendritic spikes as a mechanism for cooperative long-term potentiation. Nature *418*, 326–331.

Hu, H., Vervaeke, K., and Storm, J.F. (2002). Two forms of electrical resonance at theta frequencies, generated by M-current, h-current and persistent Na+ current in rat hippocampal pyramidal cells. J. Physiol. *545*, 783–805.

Huang, Y.Y., Kandel, E.R., Varshavsky, L., Brandon, E.P., Qi, M., Idzerda, R.L., McKnight, G.S., and Bourtchouladze, R. (1995). A genetic test of the effects of mutations in PKA on mossy fiber LTP and its relation to spatial and contextual learning. Cell *83*, 1211–1222.

Kamondi, A., Acsady, L., Wang, X.J., and Buzsaki, G. (1998). Theta oscillations in somata and dendrites of hippocampal pyramidal cells in vivo: activity-dependent phase-precession of action potentials. Hippocampus *8*, 244–261.

Kubota, M., Murakoshi, T., Saegusa, H., Kazuno, A., Zong, S.Q., Hu, Q.P., Noda, T., and Tanabe, T. (2001). Intact LTP and fear memory but impaired spatial memory in mice lacking Ca(v)2.3 (alpha(1E)) channel. Biochem. Biophys. Res. Commun. *282*, 242–248.

Lisman, J.E. (1999). Relating hippocampal circuitry to function: recall of memory sequences by reciprocal dentate-CA3 interactions. Neuron *22*, 233–242.

Lorincz, A., Notomi, T., Tamas, G., Shigemoto, R., and Nusser, Z. (2002). Polarized and compartment-dependent distribution of HCN1 in pyramidal cell dendrites. Nat. Neurosci. *5*, 1185–1193.

Ludwig, A., Budde, T., Stieber, J., Moosmang, S., Wahl, C., Holthoff, K., Langebartels, A., Wotjak, C., Munsch, T., Zong, X., et al. (2003). Absence epilepsy and sinus dysrhythmia in mice lacking the pacemaker channel HCN2. EMBO J. *22*, 216–224.

Lupica, C.R., Bell, J.A., Hoffman, A.F., and Watson, P.L. (2001). Contribution of the hyperpolarization-activated current (I(h)) to membrane potential and GABA release in hippocampal interneurons. J. Neurophysiol. *86*, 261–268.

Maccaferri, G., and McBain, C.J. (1996). The hyperpolarization-activated current (Ih) and its contribution to pacemaker activity in rat CA1 hippocampal stratum oriens-alveus interneurones. J. Physiol. *497*, 119–130.

Magee, J.C. (1998). Dendritic hyperpolarization-activated currents modify the integrative properties of hippocampal CA1 pyramidal neurons. J. Neurosci. *18*, 7613–7624.

Magee, J.C. (1999). Dendritic Ih normalizes temporal summation in hippocampal CA1 neurons. Nat. Neurosci. *2*, 508–514.

Magee, J.C., and Johnston, D. (1997). A synaptically controlled, associative signal for Hebbian plasticity in hippocampal neurons. Science *275*, 209–213.

Malleret, G., Hen, R., Guillou, J.L., Segu, L., and Buhot, M.C. (1999). 5-HT1B receptor knockout mice exhibit increased expolaratory activity and enhanced spatial performance in the Morris water maze. J. Neurosci. *19*, 6157–6168.

Malleret, G., Haditsch, U., Genoux, D., Jones, M.W., Bliss, T.V., Vanhoose, A.M., Weitlauf, C., Kandel, E.R., Winder, D.G., and Mansuy, I.M. (2001). Inducible and reversible enhancement of learning, memory, and long-term potentiation by genetic inhibition of calcineurin. Cell *104*, 675–686.

Markram, H., Lubke, J., Frotscher, M., and Sakmann, B. (1997). Regulation of synaptic efficacy by coincidence of postsynaptic APs and EPSPs. Science *275*, 213–215.

Meiri, N., Ghelardini, C., Tesco, G., Galeotti, N., Dahl, D., Tomsic, D., Cavallaro, S., Quattrone, A., Capaccioli, S., Bartolini, A., and Alkon, D.L. (1997). Reversible antisense inhibition of Shaker-like Kv1.1 potassium channel expression impairs associative memory in mouse and rat. Proc. Natl. Acad. Sci. USA *94*, 4430–4434.

Milner, B., Squire, L.R., and Kandel, E.R. (1998). Cognitive neuroscience and the study of memory. Neuron *20*, 445–468.

Nolan, M.F., Malleret, G., Lee, K.H., Gibbs, E., Dudman, J.T., Santoro, B., Yin, D., Thompson, R.F., Siegelbaum, S.A., Kandel, E.R., and Morozov, A. (2003). The hyperpolarization-activated HCN1 channel is important for motor learning and neuronal integration by cerebellar Purkinje cells. Cell *115*, 551–564.

Notomi, T., and Shigemoto, R. (2004). Immunohistochemical localization of Ih channel subunits, HCN1–4, in the rat brain. J. Comp. Neurol. *471*, 241–276.

Otmakhova, N.A., and Lisman, J.E. (2004). Contribution of Ih and GABAB to synaptically induced afterhyperpolarizations in CA1: A brake on the NMDA response. J. Neurophysiol. *92*, 2027–2039.

Otmakhova, N.A., Otmakhov, N., and Lisman, J.E. (2002). Pathway-specific properties of AMPA and NMDA-mediated transmission in CA1 hippocampal pyramidal cells. J. Neurosci. *22*, 1199–1207.

Pike, F.G., Goddard, R.S., Suckling, J.M., Ganter, P., Kasthuri, N., and Paulsen, O. (2000). Distinct frequency preferences of different types of rat hippocampal neurones in response to oscillatory input currents. J. Physiol. *529*, 205–213.

Remondes, M., and Schuman, E.M. (2002). Direct cortical input modulates plasticity and spiking in CA1 pyramidal neurons. Nature *416*, 736–740.

Robinson, R.B., and Siegelbaum, S.A. (2003). Hyperpolarization-activated cation currents: from molecules to physiological function. Annu. Rev. Physiol. *65*, 453–480.

Routtenberg, A., Cantallops, I., Zaffuto, S., Serrano, P., and Namgung, U. (2000). Enhanced learning after genetic overexpression of a brain growth protein. Proc. Natl. Acad. Sci. USA *97*, 7657–7662.

Sanes, J.R., and Lichtman, J.W. (1999). Can molecules explain long-term potentiation? Nat. Neurosci. *2*, 597–604.

Santoro, B., Grant, S.G., Bartsch, D., and Kandel, E.R. (1997). Interactive cloning with the SH3 domain of N-src identifies a new brain

specific ion channel protein, with homology to eag and cyclic nucleotide-gated channels. Proc. Natl. Acad. Sci. USA *94*, 14815–14820.

Santoro, B., Chen, S., Luthi, A., Pavlidis, P., Shumyatsky, G.P., Tibbs, G.R., and Siegelbaum, S.A. (2000). Molecular and functional heterogeneity of hyperpolarization-activated pacemaker channels in the mouse CNS. J. Neurosci. *20*, 5264–5275.

Strohmann, B., Schwarz, D.W., and Puil, E. (1994). Subthreshold frequency selectivity in avian auditory thalamus. J. Neurophysiol. *71*, 1361–1372.

Tang, Y.P., Shimizu, E., Dube, G.R., Rampon, C., Kerchner, G.A., Zhuo, M., Liu, G., and Tsien, J.Z. (1999). Genetic enhancement of learning and memory in mice. Nature *401*, 63–69.

Ulens, C., and Tytgat, J. (2001). Functional heteromerization of HCN1 and HCN2 pacemaker channels. J. Biol. Chem. *276*, 6069–6072.

Wang, Z., Xu, N.L., Wu, C.P., Duan, S., and Poo, M.M. (2003). Bidirectional changes in spatial dendritic integration accompanying long-term synaptic modifications. Neuron *37*, 463–472.

Williams, S.R., and Stuart, G.J. (2000). Site independence of EPSP time course is mediated by dendritic I(h) in neocortical pyramidal neurons. J. Neurophysiol. *83*, 3177–3182.

Williams, S.R., and Stuart, G.J. (2003). Voltage- and site-dependent control of the somatic impact of dendritic IPSPs. J. Neurosci. *23*, 7358–7367.

Witter, M.P., Wouterlood, F.G., Naber, P.A., and Van Haeften, T. (2000). Anatomical organization of the parahippocampal-hippocampal network. Ann. N Y Acad. Sci. *911*, 1–24.

Xu, C., Datta, S., Wu, M., and Alreja, M. (2004). Hippocampal theta rhythm is reduced by suppression of the H-current in septohippocampal GABAergic neurons. Eur. J. Neurosci. *19*, 2299–2309.